

Properties of Josephson junctions with amorphous-silicon interlayers

A. L. Gudkov, M. Y. Kupriyanov, and K. K. Likharev

(Submitted 2 February 1988)

Zh. Eksp. Teor. Fiz. **94**, 319–332 (July 1988)

We describe the principal results of detailed investigations of the transport properties and structure of edge-type Nb- α Si-Nb Josephson junctions. We show that the junction conductivity, notwithstanding its anomalously low value, is direct (non-tunneling) and has a most unusual (nonmonotonic) dependence on the interlayer thickness. These features can be attributed to the resonant nature of the current passing through interlayers having abrupt plane-parallel boundaries.

1. INTRODUCTION

Experimental investigations of the Josephson effect in structures having semiconducting interlayers are the subject of a rather large number of papers (see, e.g., their review in Chap. 7 of Ref. 1). Most studies, however, deal with interlayers with low free-carrier density, which behave at low temperature like ordinary tunnel barriers.² Of considerably greater physical and applied interest are structures with “direct” (non-tunneling) conduction.³

Structures of this type were developed and investigated in Refs. 4–6 with strongly doped single-crystals as the basis. The use of single crystals, however, complicates the geometry of the Josephson junctions and does not permit as yet reproducible preparation of such structures and investigations of their properties. A more realistic approach, using a standard “sandwich” geometry with an amorphous doped semiconductor as the interlayer, was used in Refs. 7 and 8. Even there, however, the required reproducibility of the junction parameters was not attained.

One of us (A. G.) has recently developed a procedure for relatively reproducible preparation of edge junctions with direct conduction, using interlayers of strongly doped silicon.⁹ Such a reproducibility has made it possible to use these junctions to solve many important applied problems, so that a detailed investigation of their structure and of their electrophysical properties has become more timely. In the present paper we report the results of these investigations and draw conclusions concerning the conduction mechanism in these junctions.

2. JUNCTION PREPARATION

A diagram of the cross section of the investigated structures is shown in Fig. 1a. The substrates were standard single-crystal Si slabs. After a preliminary surface treatment of the slab with Ar ions (to improve the adhesion), it was coated by the ion-plasma method with the first Nb^I film of thickness $t = 250$ nm. This film was covered with an insulating Al₂O₃ layer, on which was produced, by usual photolithography, a mask having the shape desired for the lower electrode. The remaining uncoated sections of the Nb^I film were removed by ion-chemical etching in a freon-oxygen mixture: this produced on the remaining part of the film edges with angle $\alpha \approx 70^\circ$ to the slab surface (Fig. 1a). The surfaces of these edges were thoroughly cleaned with Ar ions. Observations in a raster electron microscope have shown that these operations make the niobium surface atom-smooth.

Immediately after the cleaning (without breaking the vacuum), the resultant structure was coated, by ion-plasma

sputtering from a single-crystal target in an Ar atmosphere, with a layer of amorphous silicon (α -Si) about 3–15 nm thick and with a second layer of niobium (Nb^{II}) about 250 nm thick. The last step in the junction preparation was formation, by photolithography and by ion-chemical methods, of an Nb^{II} upper electrode of the desired shape. This shape was chosen such that the upper electrode overlapped slightly the lower, with overlap width w from 1 to 4 μm (Fig. 1b: Fig. 1a shows the cross section of just such a section). An edge Josephson Nb^I – α -Si – Nb^{II} junction was produced on each such section, with area $S = wt / \cos \alpha$ amounting to fractions of a square micron.

3. PRINCIPAL ELECTROPHYSICAL PROPERTIES OF THE JUNCTIONS

3.1. *Current-voltage characteristics (IVC)*. Figure 2 shows a typical family of dc IVC plotted in the temperature range $0.6 \leq T/T_c \leq 1$ (measurements at $T > T_c$ are made difficult by the high resistance of the niobium electrodes). The main features of these characteristics are:

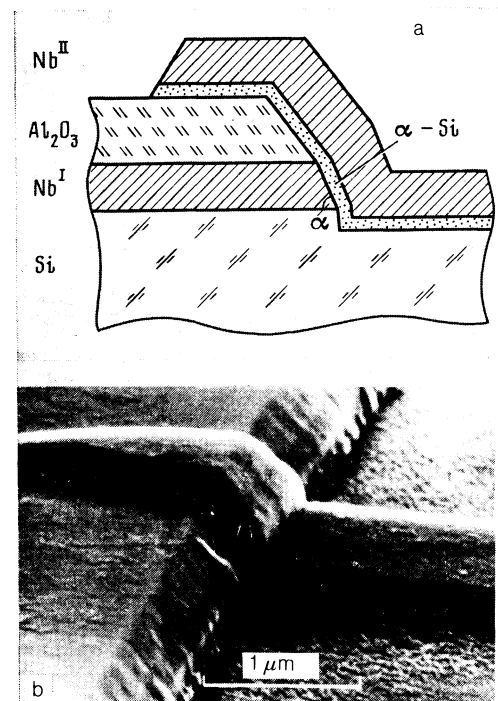


FIG. 1. Cross section through an edge junction (a) and its image in a raster electron microscope (b).

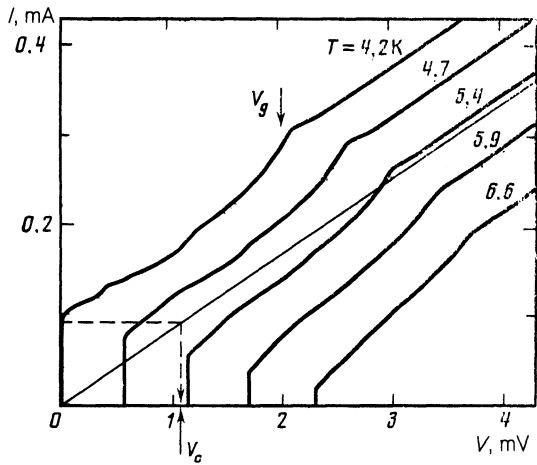


FIG. 2. Current-voltage characteristics of typical junction ($d = 5$ nm, $S = 0.6 \mu\text{m}^2$) at various temperatures.

a. Absence of hysteresis from the IVC, attesting to small (less than unity) values of the capacitance parameter $\beta_c = (2e/\hbar)I_c R_N^2 C$ (see Ref. 10, Chap. 4); in fact, estimates of the capacitance C based on the junction dimensions and on the known value $\epsilon_{\text{Si}} \sim 10$ yield for β_c values from 0.1 to 1.

b. Relatively high (up to 1 mV) values of the "characteristic voltage" $V_c \equiv I_c R_N$.

c. A noticeable "gap" singularity at a voltage $V_g = [\Delta^I(T) + \Delta^{II}(T)]/e$ of order 1.8 mV.

d. An appreciable "excess" direct current $I_{\text{ex}} = I - V/R_N$ at voltages $V \gg V_g$, a current typical of Josephson junctions with direct conductivity.

e. Onset, under microwave irradiation, of a large number of Josephson current steps (see Fig. 2 of Ref. 9), with a

behavior close to that following from the simple resistive model (Ref. 10, Chap. 2).

In general, it should be noted that the shapes of the IVC of our junctions almost coincide with the universal shape of the IVC of superconducting small-size weak links, a form first revealed by Weitz *et al.* for ideal junctions.¹¹ Similar IVC were observed later also for other junctions with direct conduction, such as an SNS sandwich with x -Te interlayer,¹² very short bridges of variable thickness with Nb bridges,¹³ and also junctions with GeSn (Ref. 7) and α -Si (Ref. 14) interlayers. It is assumed at present that precisely such an IVC should follow from the weak-coupling model proposed by Kulik and Omelyanchuk.¹⁵ Unfortunately, the theory^{16,17} of nonstationary processes within the framework of this model has not yet reached the stage where the exact shape of the IVC can be calculated, but the value of I_{ex} calculated in these references agrees well with the experimental data, including ours.

3.2. *Temperature dependences of IVC parameters.* Possibly the most important experimental fact obtained by us is that the normal resistance of the junctions is independent of temperature (Fig. 1). This independence is observed with accuracy at least better than 1% in the interval $1.5 \text{ K} \leq T \leq T_c$ for those interlayer thicknesses ($d \leq 30$ nm) for which the junctions still exhibit a noticeable Josephson effect. This result indicates unequivocally that the impurity density in the interlayers of our junctions exceeded the critical value corresponding to an insulator-metal junction (according to the data of Ref. 18, this value for Nb is close to 11.5 at. %).

The temperature dependence of the "gap" voltage V_g turned out to be close that following from the BCS theory for symmetrical junctions ($\Delta^I = \Delta^{II} = \Delta$), but with a somewhat decreased value of the energy gap: $\Delta(0)/\Delta_{\text{BCS}}(0) = 0.8$ (see Fig. 3a). The same figure shows the $V_g(T)$ dependences that follow from the theory¹⁹ for two-layer SN

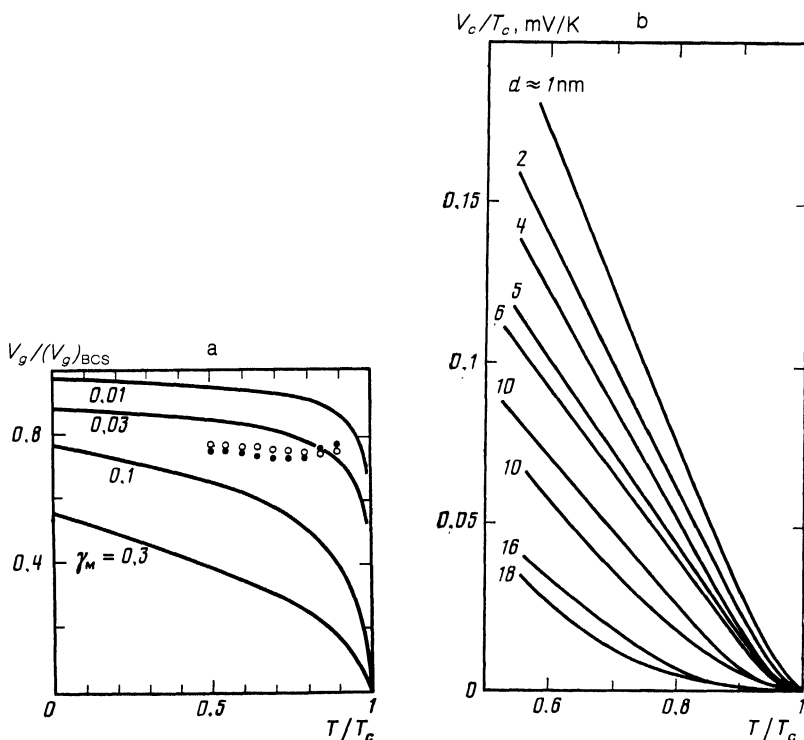


FIG. 3. Temperature dependences of the "gap" voltage $V_g = (\Delta^I + \Delta^{II})/e$ for $d = 5$ and 6 nm (a) and of the characteristic voltage $V_c = I_c R_N$ (b) for different values of d ; $\gamma_m = d\sigma\xi_s/\delta_s\xi_N$.

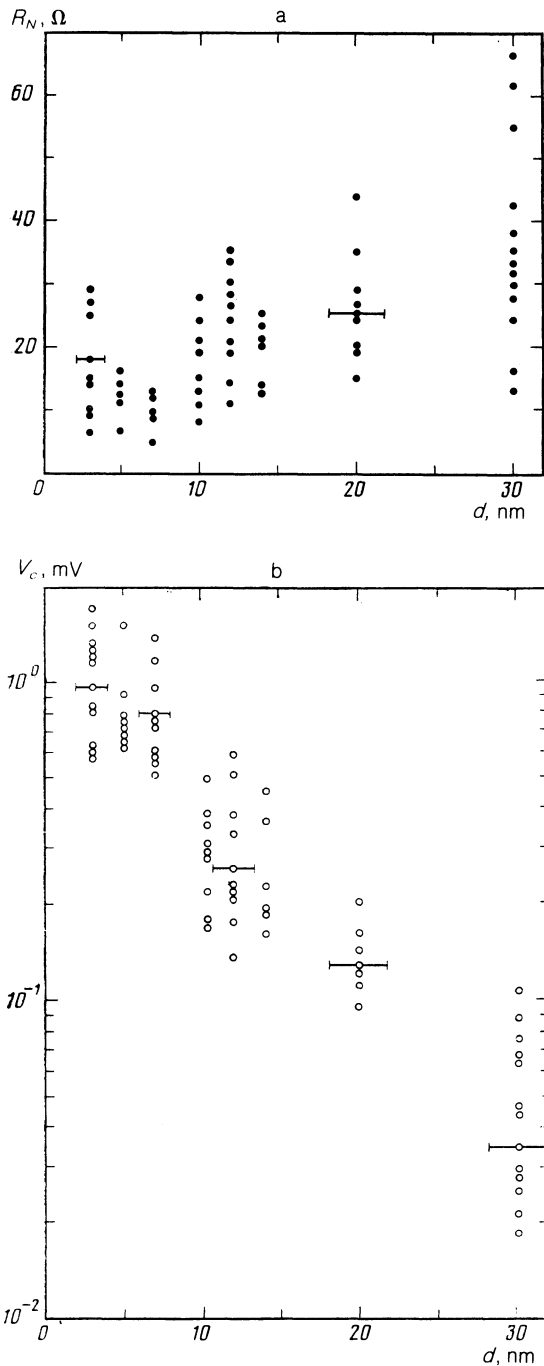


FIG. 4. Normal junction resistance R_N (referred to the area $S = 0.6 \mu\text{m}^2$) (a) and junction characteristic voltage V_c (b) vs the thickness of the α -Si interlayer at a temperature 4.2 K.

films. The great difference between the character of these temperature dependences prevents us from attributing the observed decrease of $\Delta(0)$ to the simple effect of proximity of Nb to some thin normal layer on its interface with α -Si.

Figure 3b shows the temperature dependences of the characteristic voltage V_c for a number of junctions with various interlayer thicknesses. They are qualitatively close to those following from the theories of SNS-type structures with dirty³ or pure¹⁹ interlayers, especially following substitution in them of the experimental $\Delta(0)$ value. An exception

is the region $T \approx T_c$, where the experimental curves lie systematically lower than the theoretical. This difference can be fully attributed to suppression of the critical current by pickup from the measurement circuits (Ref. 10, Chaps. 2–4), which is particularly noticeable in the region $T \rightarrow T_c$, where the values of I_c are small (several or tens of microamperes).

3.3. *Dependence of the parameters on the interlayer thickness.* Figure 4 shows plots of R_N and V_c against the interlayer thickness d , the latter calculated from the known average rate of deposition of the α -Si and from the duration of this process. Unfortunately, the scatter, due to non-uniformity, of the real values of d and of the junctions located in different sections of even one interlayer (of 76 mm diameter) was quite large (about 20%). This made it possible to use the data of Fig. 4 only to determine the principal tendencies of the $R_N(d)$ and $V_c(d)$ dependences. Namely, V_c and R_N exhibit no systematic variation with thickness up to $d \sim 10$ nm, after which R_N begins to grow and V_c begins to decrease approximately exponentially: $V_c \propto \exp\{d/d_0\}$ with the parameter d_0 ranging from 6 to 10 nm.

Since the constancy of the function $R_N(d)$ for small d contradicted all the heretofore known Josephson-junction models, we performed additional measurements of the $R_N(d)$ and $I_c(d)$ dependences on a subset of junctions located on like sections of the substrates. The results of these measurements (Fig. 5) are evidence not only that R_N does not increase in general with increase of d (for $d > 10$ nm), but also that $R_N(d)$ and $I_c(d)$ are oscillating functions.

3.4. *Influence of magnetic field.* Figure 6a shows the influence of an external magnetic field normal to the substrate plane on the shape of the IVC of a typical junction and on its critical current. It is clearly seen that the current in the region $|V| < V_g$ is close to the normal value V/R_N even if the critical current is completely suppressed by the field. This behavior is typical of junctions with direct conductivity.³

Plots of $I_c(H)$ are shown in Fig. 6b for two junctions of different width w . It can be seen that these plots are close in shape to the usual "diffraction" plots ($I_c(H) \propto \sin x/x$, $x \propto H$). Note that no exact coincidence should actually not take place here, in view of the nonplanar geometry of the junction (to our knowledge, no rigorous calculation was made for this geometry even in the limit $w \ll \lambda_J$). At any rate, the experimental dependences indicate unequivocally that the linear density of the critical-current $J_c = j_c t / \cos \alpha$ is practically constant over the junction width w , and excludes the possibility that the conduction is via random microshorts.

Additional proofs of the macroscopic uniformity of the junctions were obtained by measuring the behavior, in a magnetic field, of a system of two identical junction close to each other and connected in parallel (Fig. 7a). The resultant interference-diffractive picture (Fig. 7b) points, in particular, to near-equality of the values of these junctions, which practically unlikely if microshorts are present.

Even more convincing are the results shown in Fig. 8. The critical currents I_c of closely lying junctions of identical form turn out to be so close ($\delta I_c / I_c \leq 3\%$), that when they are connected in series the resultant IVC do not permit even resolution of their successive transitions into the resistive

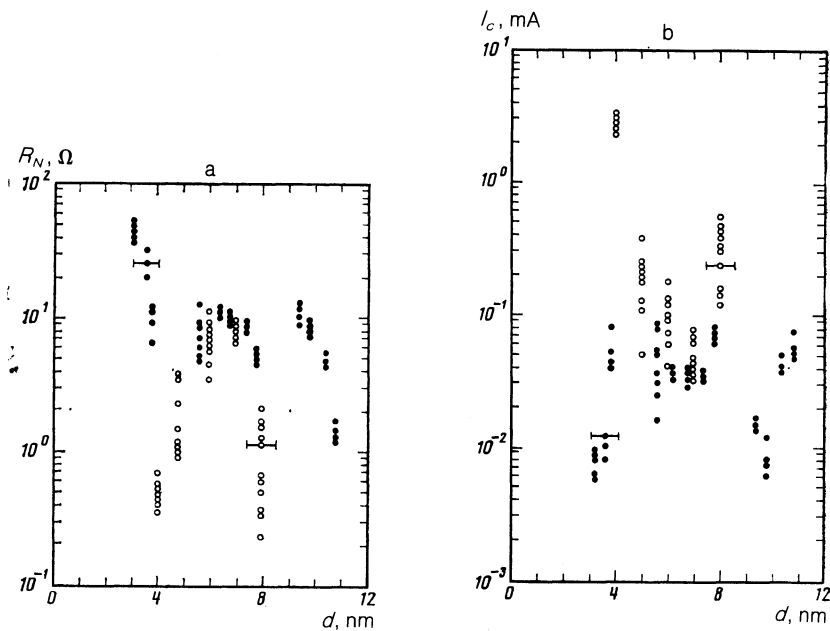


FIG. 5. Dependences of $R_N(d)$ and $I_c(d)$ (b) for junctions located on like sections (measuring about 2 cm^2) of substrates, for two independent experiments with different sets of α -Si interlayer thickness. The data are referred to an area $S = 1 \mu\text{m}^2$.

state (Fig. 8b). When such a system is irradiated by an intense microwave ($f = 37 \text{ GHz}$), the positions of the edges of the produced Josephson current steps practically coincide. As a result, the "summary" IVC reveals only collective current steps at voltages $V = V_n = nN(h/2e)f$ ($N = 11$, Fig. 8a).

4. SUPPLEMENTARY STRUCTURAL INVESTIGATIONS

To gain an even closer insight into the structure of the junction sublayer and its interfaces with the electrodes, we have performed a number of supplementary investigations of planar two- and three-layer structures having relatively large area and prepared under the same conditions as the edge junctions.

4.1. $R_N(d)$ dependence at large thicknesses. At $d \geq 30 \text{ nm}$, the resistance of the three-layer structures $\text{Nb}^{\text{I}} - \alpha\text{-Si} - \text{Nb}^{\text{II}}$ rises approximately exponentially, and increases by an order of magnitude for each increase $\Delta d \approx 50 \text{ nm}$. In this case, R_N increases with rise of temperature.

This behavior agrees with the result described in Ref. 20 for $\text{Nb} - \text{SiO}_x - \alpha\text{-Si} - \text{SiO}_x - \text{Pb}$ structures for smaller d (a value $d = 30 \text{ nm}$ is cited there), and corresponds apparently to the hopping conduction of almost undoped amorphous silicon (see, e.g., Ref. 21, Chap. 2). This shows once

more that the resistance R_N of our junctions is in principle different ($d \leq 15 \text{ nm}$) in the "working" thickness range (Figs. 4a and 5).

4.2. Auger-spectroscopy investigations of three-layer structures of the same type have shown that the working region d of the sublayer contains an appreciable tungsten concentration (1–3 at.%). Even higher concentrations (up to 20 at.% at $d \approx 10 \text{ nm}$) are obtained by this method for niobium, but this figure can be regarded only as an upper bound, since an appreciable part of the signal in the spectra can be due to nonuniformity of the layer-by-layer etching of the planar structure.

4.3. Electron microscopy. We have also investigated the transverse section of a three-layer structure with $d \approx 1 \text{ nm}$ with a transmission electron microscope. The investigations have shown that the interfaces of the Nb and α -Si are atomically abrupt, and the interlayer itself is atomically homogeneous.

4.4. Anodizing of a two-layer structure. Figure 9 shows the results of measurement of the longitudinal resistance (per square) of an $\alpha\text{-Si-Nb}^{\text{II}}$ structure anodized step by step in a 0.1% solution of citric acid. Since the anodizing constants $\beta = d/V$ of niobium and silicon are close in value (our measurements yielded $\beta_{\text{Nb}} \approx 0.9 \text{ nm/V}$ and $\beta_{\alpha\text{-Si}} \approx 1.3 \text{ nm/V}$), this plot can be regarded approximately as the result

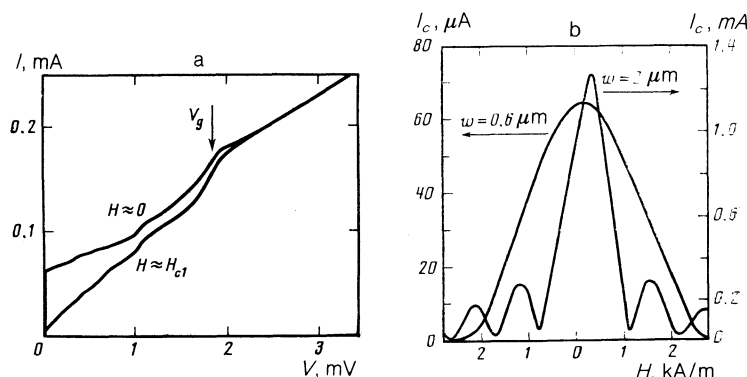


FIG. 6. Influence of the magnetic field on the shape of the current-voltage characteristic of a junction (a) and dependence of the critical currents of junctions with upper electrodes that differ in width w on the magnetic field normal to the substrate plane (b).

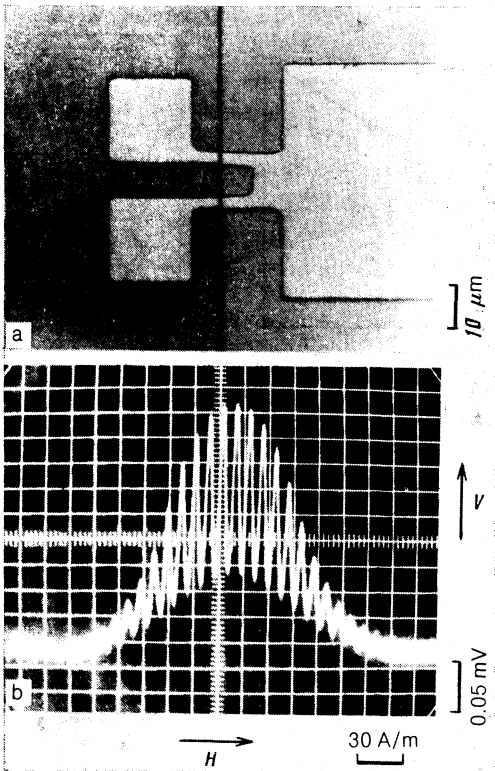


FIG. 7. Superconducting quantum interferometer consisting of two junctions: top view (a) and dependence of the voltage on the interferometer on the magnetic field normal to the substrate plane for direct current $I > I_c$ (b).

of a successive thinning of the initial structure (see the inset).

It follows from this result that an intermediate-phase layer of thickness $d \approx 6$ nm is produced between the Nb and the α -Si, differs from them in conductivity, and its boundaries with them are very abrupt. The resistivity of this layer varies little with temperature (the difference shown in Fig. 9 may be due to the shunting of the layer by the Si substrate at $T = 300$ K) and is of the order $10^{-3} \Omega \cdot \text{cm}$.

5. DISCUSSION OF RESULTS

The entire aggregate of our results shows that the interlayers of our Josephson junctions in the "working" thickness interval ($3 \text{ nm} \leq d < 15 \text{ nm}$) consist of a certain phase with metallic conductivity, separated from the niobium electrodes by atomically abrupt boundaries. The phase itself is apparently either one of the niobium silicides²² or simple a metastable solid solution of Nb (< 20 at. %) in Si.

The main paradox is that the normal resistance of our junctions per unit area ($R_N S \sim 10^{-7} \Omega \cdot \text{cm}^2$) is found to be several orders larger than given by the usual formula $R_N S = \rho_N d$, with an experimental value $\rho_N \sim 10^{-3} \Omega \cdot \text{cm}$. A resolution of this paradox, as well as an explanation of the unusual $R_N(d)$ and $I_c(d)$ dependences shown in Figs. 4a and 5, can be found by recognizing that the interlayer boundaries are atomically abrupt and practically plane-parallel. Under these conditions, a principally important role is assumed by interference between the de Broglie waves of the conduction electrons in the weak-link interlayer; this inter-

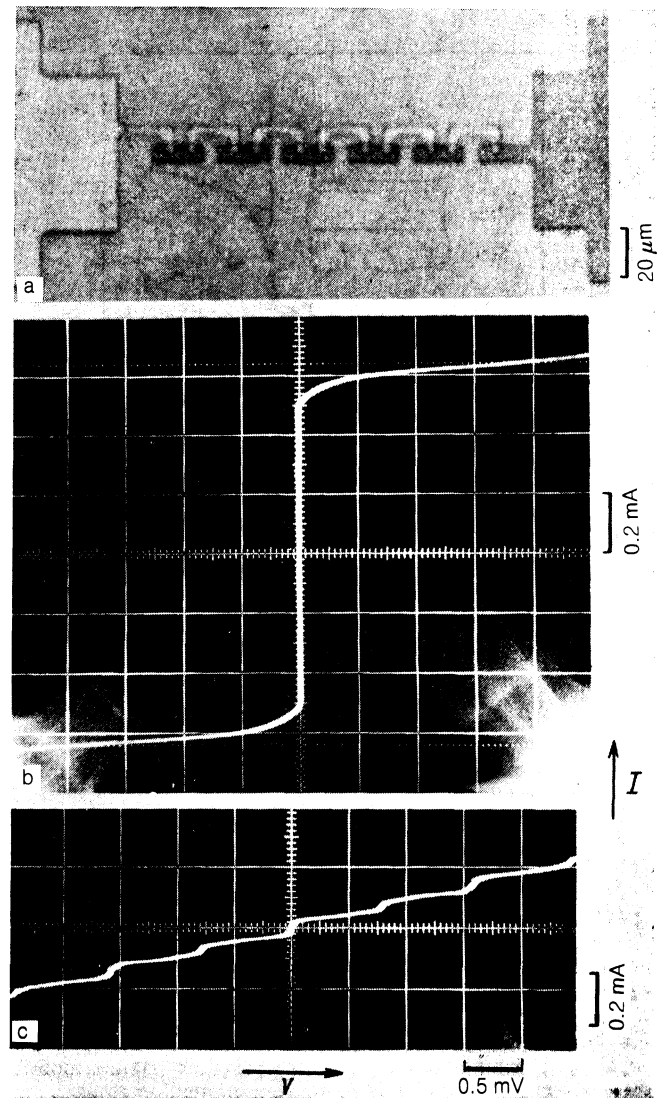


FIG. 8. Chain of $N = 11$ series-connected junctions (a) and its current-voltage characteristics in the absence (b) and in the presence (c) of a microwave field of frequency $f = 37$ GHz.

ference, to our knowledge, was not taken into account in any of the known theories of superconducting weak links.

We have calculated the properties of such "resonant" weak links by starting from the microscopic theory of superconductivity, using the following assumptions:

1. The junction is a one-dimensional structure of the type of an SNS "sandwich" of thickness d with abrupt plane-parallel boundaries.

2. The interlayer material has a spherical Fermi surface with Fermi velocity v_N that differs substantially from the Fermi velocity v_S of the electrons in the superconducting electrodes:

$$\gamma = v_N/v_S \ll 1. \quad (1)$$

3. The electrons are specularly reflected from the structure boundaries, and their mean free path l_N in the weak-link material is large compared with d :

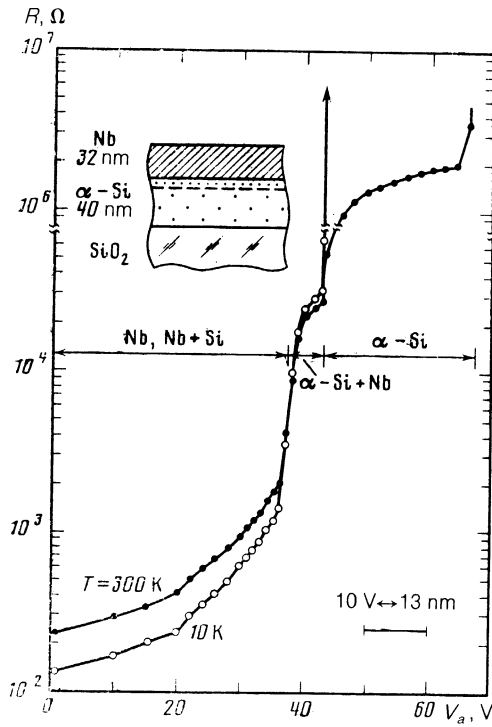


FIG. 9. Resistance of two-layer α -Si-Nb¹¹ strip 0.1 mm wide and 2 mm long vs the anodizing voltage (the inset shows a diagram of the strip cross section).

$$l_N \gg d. \quad (2)$$

The second of these assumptions is justified by the relatively large experimental value of ρ_N , and the last is the result of the low efficiency of electron scattering by inhomogeneities of atomic scale a (the de Broglie wavelength of the electrons in the interlayer is $\lambda_N \propto \lambda_S / \gamma \gg a$) and is necessary to explain the oscillations in the $R_N(d)$ dependence.

Under the foregoing assumptions it can be stated that for normal electrons ($T > T_c$) the weak-link region is a rectangular potential barrier having a width d and a low transparency $D \propto \gamma^2 \ll 1$. It is therefore possible to determine R_N by using the tunnel-theory formula²⁵ which can be represented in our case in the form

$$R_N^{-1} = 2R_0^{-1} \left[\langle xD_1(x) \rangle + \left(\frac{p_s}{p_N} \right)^2 \langle xD_2(x) \rangle \right],$$

$$R_0^{-1} = \frac{Se^2 p_N^2}{2\pi^2 \hbar^3}, \quad \langle xD_{1,2}(x) \rangle = \int_0^1 (xD_{1,2}(x)) dx. \quad (3)$$

Here S is the junction cross-section area, $p_{S,N}$ are the S - and N -metal electron Fermi momenta, and the transparency coefficients for the above-barrier (D_1) and below-barrier (D_2) reflections of the electrons equal,²⁴ accurate to terms proportional to γ^2 ,

$$D_1(x) = \left[1 + \left(\frac{\gamma}{2} \sin \left(\frac{2\pi d}{\lambda_N} x \right) \right)^2 \right]^{-1},$$

$$D_2(x) = \left[1 + \frac{1}{4x^2(1-x^2)} \text{sh}^2 \left(\frac{2\pi d}{\lambda_N} \frac{p_s}{p_N} x \right) \right]^{-1}. \quad (4)$$

The second term in (3), which takes into account the contribution made to R_N^{-1} by the electrons whose momentum component p parallel to the SN boundaries is larger than p_N , decreases exponentially with increase of d and is comparable with the first term that varies nonmonotonically with d only if $d \leq \lambda_N (p_N/p_S) \ll \lambda_N$.

The results of calculations with the aid of Eqs. (3) and (4) for three values of the parameter and for equal effective electron masses are shown in Fig. 10a. It can be seen that the resistance oscillates, having minima at thicknesses $d = k\lambda_N/2$. With increase of d , the swing of the oscillations decreases in inverse proportion to the number K of de Broglie half-waves spanned by the length d :

$$\Delta R_N = \frac{4}{\gamma K} R_0, \quad (5)$$

while R_N tends to the value of the resistance produced by one of the boundaries

$$R_N = {}^{3/4} \gamma R_0. \quad (6)$$

Proceeding to an analysis of the superconducting properties of the structure, we assume in addition that the critical temperature of the interlayer material is $T_{cN} = 0$. In this case the anomalous $F(r_1, r_2)$ and normal $G(r_1, r_2)$ Gor'kov functions that describe the weak-link superconducting properties vary over the coherence length of the material like $\xi_N = \hbar v_N / 2\pi T$. At $d \sim \xi_N$, therefore, the properties of the

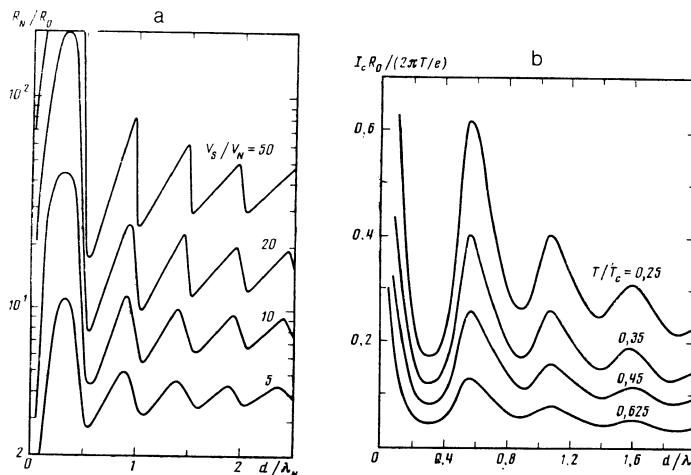


FIG. 10. Theoretical $R_N(d)$ dependence (a), neglecting scattering, for different ratios of the electron Fermi velocities in the electrodes and interlayer, and theoretical $I_c(d)$ dependence (b) for different temperatures at $v_S/v_N = 5$.

structure can no longer be described with the aid of the transparency coefficients D_1 and D_2 , the tunnel-theory equations are not valid, and all the calculations must be carried out in the framework of the Gor'kov equations.²⁵

The solution of these equations in the N region reduces, by virtue of condition (2) and the assumption $T_{cN} = 0$, to the solution of a system of differential equations with constant coefficients, and can be represented in the form of a superposition of plane waves incident on and reflected from the boundaries. The solution in the S region can also be represented as a superposition of plane waves, for as a result of (1) the modulus of the order parameter and the Gor'kov equations $F(r_1, r_1)$ and $G(r_1, r_1)$ integrated over the Fermi surface, which describe the electron scattering, can be regarded, accurate to terms proportional to γ^2 , as independent of the spatial coordinates. Determining the amplitudes of the plane waves from the conditions that the functions F and G and their derivatives be continuous on the structure boundaries, and substituting the solution obtained in this manner in the equation for the supercurrent I_s , we obtain the following dependence of I_s on the phase difference of the electrode order parameters:

$$I_s R_N = \frac{4\pi T}{e} \sum_{\omega=0}^{\infty} \left\langle 8\Delta^2 \sin \varphi x^3 \left[8x^2 \Delta^2 \cos^2 \frac{\varphi}{2} + \gamma^2 E (\omega + E) \sin^2 \left(\frac{2\pi d}{\lambda_N} x \right) + 2(\gamma E \operatorname{sh} b + 2\omega x \operatorname{ch} b)^2 \right]^{-1} \right\rangle$$

$$b = \frac{d}{2\xi_N x} \frac{\omega}{\pi T}, \quad E = (\omega^2 + \Delta^2)^{1/2}, \quad (7)$$

where $\omega = \pi T(2n + 1)$ are Matsubara frequencies. At small sublayer thicknesses, $d \ll \xi_N, \lambda_N$, Eq. (6) leads to the theoretical result of Ref. 15, and for $d < \xi_N/\gamma$ and $T \approx T_c$ expressions (3) and (4) go over into the Aslamazov-Larkin equation²⁶

$$I_s R_N = \frac{\pi}{4} \frac{\Delta^2}{eT} \sin \varphi \quad (8)$$

for arbitrary ratio of d and λ_N .

Numerical calculations using Eq. (7) with $\lambda_N = \xi_N/2$ (see Fig. 10b) attest to the nonmonotonic character of the $I_c(d)$ dependence. The period of the oscillations is the same as of the function $R_N(d)$, but the swing of the oscillations decreases exponentially with increase of d , and turns out to be exponentially small at $d \gg \xi_N$. The parameter V_c , increasing with increase of d from zero at $d = 0$ to its maximum value at $d \approx \xi_N/\gamma$, decreases practically monotonically with further increase of d . The $V_c(T)$ dependences (Fig. 11) are qualitatively close to those calculated earlier for pure weak bonds with planar transparent boundaries.²⁷

Comparison of Figs. 3 and 11 shows that the experimental and theoretical $V_c(T)$ dependences at $d < 10$ nm agree well if it is assumed that $\xi_N \approx 10$ nm. According to (3) this yields $v_N \sim 10^7$ cm/s, leading to the reasonable value $\gamma \sim 5$. Next, assuming the effective carrier mass in α -Si to be close to m_0 (with allowance for the fact that impurities such as Nb and W usually have deep levels in Si), we have for the de Broglie wavelength the estimate $\lambda_N \sim 6$ nm. This is practically equal to the value of λ_N that follows from the period $\Delta d = \lambda_N/2$ of the oscillations of the $R_N(d)$ and $I_c(d)$ dependences.

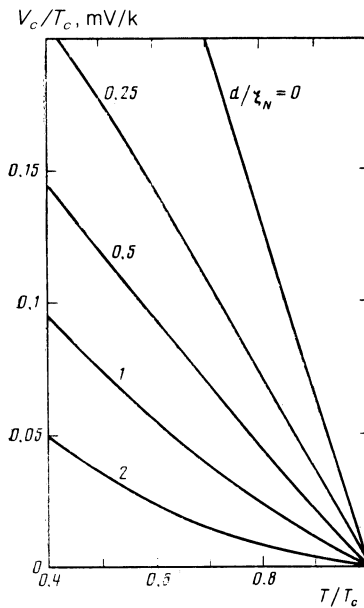


FIG. 11. Theoretical temperature dependences of the characteristic voltage $V_c(T)$ for various values of the ratio d/ξ_N at $v_S/v_N = 5$ and $\xi_N/\lambda = 2$.

6. CONCLUSION

Thus, the proposed "resonance" model of a Josephson junction is in reasonable semiquantitative agreement with all the experimental results. The most important here is its ability to explain the anomalously large values of R_N and the unusual (nonmonotonic) $R_N(d)$ dependence. According to this model, all the transport properties of the structure are connected with the processes of reflection of electrons from the interface of the metals (Nb and strongly doped α -Si), which have greatly differing Fermi velocities. In this case a specific interference takes place in the interlayer between de Broglie waves, for which the junction plays the role of a resonator of the Fabry-Perot type.

It is possible that similar phenomena have occurred in the experiments with the very similar planar junctions described in Ref. 14 (although its authors believe that their results can be explained using resonance-tunneling premises), and also in the just received Ref. 28. The answer to this question requires additional study of the properties of these junctions, primarily the details of the $R_N(d)$ dependence. Similar investigations are all the more relevant, since α -Si interlayers are apparently quite promising for the development of Josephson junctions with electrodes of ceramic high-temperature superconductors.

The authors thank V. I. Makhov for support and interest.

¹A. Barone and G. Paterno, *Physics and Applications of the Josephson Effect*, Wiley, 1982.

²L. G. Aslamazov and M. V. Fistul', Zh. Eksp. Teor. Fiz. **81**, 382 (1981) [Sov. Phys. JETP **54**, 206 (1981)].

³K. K. Likharev, Rev. Mod. Phys. **51**, 101 (1979).

⁴C. L. Huang and T. van Duzer, Appl. Phys. Lett. **25**, 753 (1974).

⁵M. Schyfter, J. Maah-Sango, N. Raley, et al., IEEE Trans. MAG-13, 862 (1977).

⁶A. L. Gudkov, Yu. E. Zhuravlev, V. I. Makhov, and A. V. Tyablikov,

- Pis'ma Zh. Tekh. Fiz. **9**, 1061 (1983) Sov. J. Tech Phys. Lett. **9**, 457 (1983)].
- ⁷E. L. Hu, L. D. Jackel, A. R. Strnad, *et al.*, Appl. Phys. Lett. **32**, 584 (1978).
- ⁸A. L. Gudkov, V. I. Makhov, A. N. Samus', and A. V. Tyablikov, Pis'ma Zh. Tekh. Fiz. **7**, 502 (1981) Sov. J. Tech. Phys. Lett. **7**, (1981)].
- ⁹A. L. Gudkov, K. K. Likharev, and V. I. Makhov, *ibid.* **11**, 1423 (1985) [**11**, 587 (1985)].
- ¹⁰K. K. Likharev, *Introduction to the Dynamics of Josephson Junctions* [in Russian], Nauka, 1985, Chap. 4.
- ¹¹D. A. Witz, W. J. Skocpol, and M. Tinkham, J. Appl. Phys. **49**, 4873 (1978).
- ¹²K. Nagata, S. Uehara, A. Matsuda, and H. Takayanagi, IEEE Trans. **MAG-17**, 771 (1981).
- ¹³H. Ohta, IEEE Trans. **ED-27**, 2027 (1980).
- ¹⁴V. N. Gubankov, S. A. Kovonyuk, and V. P. Koshelets, Zh. Eksp. Teor. Fiz. **89**, 1335 (1985) Sov. Phys. JETP **62**, 773 (1985).
- ¹⁵I. O. Kulik and A. N. Omel'yanchuk, Pis'ma Zh. Eksp. Teor. Fiz. **21**, 216 (1975) JETP Lett. **21**, 96 (1975)]. Fiz. Nizk. Temp. **3**, 945 (1977) [Sov. J. Low Temp. Phys. **3**, 459 (1977)].
- ¹⁶S. N. Artemenko, A. F. Volkov, and A. V. Zaitsev, Zh. Eksp. Teor. Fiz. **76**, 1816 (1979) [Sov. Phys. JETP **49**, 924 (1979)].
- ¹⁷A. V. Zaitsev, *ibid.* **78**, 221 (1980) [**51**, 111 (1980)].
- ¹⁸G. Hertel, D. J. Bishop, E. G. Spencer, *et al.*, Phys. Rev. Lett. **50**, 743 (1983).
- ¹⁹A. A. Golubov, M. Yu. Kupriyanov, and V. F. Lukachev, Mikroelektronika **12**, 342 (1983).
- ²⁰M. R. Beasley, S. Bending, and J. Grayleal, Localizat. Interact. and Transp. Phenom., Proc. Int. Conf. Brauschweig, Aug. 23-28, 1984, Berlin, 1985, p. 138.
- ²¹N. F. Mott and E. A. Davis, *Electronic Processes in Non-Crystalline Materials*, Oxford, 1971.
- ²²*Superconducting Compounds of Transition Metals* [in Russian], Nauka, 1976.
- ²³I. O. Kulik and I. K. Yanson, *Josephson Effect in Superconducting Tunneling Structure*, Halsted, 1972, Chap. 1.
- ²⁴S. Flugge, *Practical Quantum Mechanics*, Vol. 1, Springer, 1971.
- ²⁵A. A. Abrikosov, L. P. Gor'kov, and I. E. Dzyaloshinskii, *Quantum Field-Theoretical Methods in Statistical Physics*, Pergamon, 1965.
- ²⁶L. G. Aslamazov and A. T. Larkin, Pis'ma Zh. Eksp. Teor. Fiz. **9**, 150 (1969) [JETP Lett. **9**, 87 (1969)].
- ²⁷M. Yu. Kupriyanov, Fiz. Nizk. Temp. **7**, 700 (1981) [Sov. J. High Temp. Phys. **7**, (1981)].
- ²⁸A. S. Barrera and M. R. Peasley, Preprint, 1987.

Translated by J. G. Adashko